



Harmine Alleviates Titanium Particle-Induced Inflammatory Bone Destruction by Immunomodulatory Effect on the Macrophage Polarization and Subsequent Osteogenic Differentiation

OPEN ACCESS

Edited by:

Teun J. De Vries,
VU University Amsterdam,
Netherlands

Reviewed by:

Katharina F. Kubatzky,
Heidelberg University, Germany
Astrid Diana Bakker,
VU University Amsterdam,
Netherlands

*Correspondence:

Yuji Wang
yujwang@sohu.com
Ruixia Zhu
392849984@qq.com
Dechun Geng
szgengdc@163.com

†These authors have contributed
equally to this work

Specialty section:

This article was submitted to
Inflammation,
a section of the journal
Frontiers in Immunology

Received: 23 January 2021

Accepted: 26 April 2021

Published: 17 May 2021

Citation:

Wang L, Wang Q, Wang W, Ge G,
Xu N, Zheng D, Jiang S, Zhao G,
Xu Y, Wang Y, Zhu R and Geng D
(2021) Harmine Alleviates Titanium
Particle-Induced Inflammatory Bone
Destruction by Immunomodulatory
Effect on the Macrophage
Polarization and Subsequent
Osteogenic Differentiation.
Front. Immunol. 12:657687.
doi: 10.3389/fimmu.2021.657687

Liangliang Wang^{1†}, Qing Wang^{2†}, Wei Wang^{2†}, Gaoran Ge², Nanwei Xu¹, Dong Zheng¹,
Shijie Jiang¹, Gongyin Zhao¹, Yaozeng Xu², Yuji Wang^{1,3,4*}, Ruixia Zhu^{1*}
and Dechun Geng^{2*}

¹ Department of Orthopaedics, The Affiliated Changzhou No. 2 People's Hospital of Nanjing Medical University, Changzhou, China, ² Department of Orthopaedics, The First Affiliated Hospital of Soochow University, Suzhou, China,

³ Departments of Orthopedic Surgery and Biochemistry and Molecular Biology, Mayo Clinic, Rochester, MN, United States,

⁴ Department of Orthopedics, The Third Affiliated Hospital of Gansu University of Chinese Medicine, Baiyin, China

Peri-prosthetic osteolysis (PPO) and following aseptic loosening are regarded as the prime reasons for implant failure after joint replacement. Increasing evidence indicated that wear-debris-irritated inflammatory response and macrophage polarization state play essential roles in this osteolytic process. Harmine, a β -carboline alkaloid primitively extracted from the *Peganum harmala* seeds, has been reported to have various pharmacological effects on monoamine oxidase action, insulin intake, vasodilatation and central nervous systems. However, the impact of harmine on debris-induced osteolysis has not been demonstrated, and whether harmine participates in regulating macrophage polarization and subsequent osteogenic differentiation in particle-irritated osteolysis remains unknown. In the present study, we investigated the effect of harmine on titanium (Ti) particle-induced osteolysis *in vivo* and *in vitro*. The results suggested harmine notably alleviated Ti particle-induced bone resorption in a murine PPO model. Harmine was also found to suppress the particle-induced inflammatory response and shift the polarization of macrophages from M1 phenotypes to M2 phenotypes *in vivo* and *in vitro*, which improved anti-inflammatory and bone-related cytokines levels. In the conditioned medium from Ti particle-stimulated murine macrophage RAW264.7 cells treated with harmine, the osteoblast differentiation ability of mouse pre-osteoblastic MC3T3-E1 cells was greatly increased. And we also provided evidences that the immunomodulatory capacity of harmine might be attributed to the inhibition of the c-Jun N-terminal kinase (JNK) in wear particle-treated macrophages. All the results strongly show that harmine might be a promising therapeutic agent to treat PPO.

Keywords: peri-prosthetic osteolysis, chronic inflammation, harmine, macrophage polarization, osteoimmunomodulatory

INTRODUCTION

Total joint arthroplasty (TJA) is becoming more successful and minimally invasive to treat severe joint disease (1, 2). TJA relieves pain symptoms effectively and improves the quality of patients' daily life. However, despite advancement in surgical skills, materials and implant designs, a risk of aseptic loosening is still exist, which leads to peri-prosthetic osteolysis (PPO). Increasing evidence shows that peri-prosthetic inflammatory bone destruction initiated by debris mainly leads to arthroplasty failure (3, 4).

Wear debris shed from joint prostheses is generated by mechanical impact and biological responses, besides polymeric, metallic, ceramic debris, etc. (5–7). These particles induce a chronic inflammation response by the further recruitment of macrophages, which secrete multiple proinflammatory factors, such as chemokines, and cytokines (8, 9). Macrophages are critical in the periprosthetic inflammatory process. Moreover, increasing evidence has demonstrated that macrophage polarization exerts great influence in the pathogenesis of inflammatory osteolysis (10–12). For the past few years, the concept of M1 macrophages (marked by CD86 and inducible nitric oxide synthase (iNOS)) and M2 macrophages (marked by CD206 and arginase-1 (Arg-1)) has been built (13). M1 macrophages can be irritated by microbial products or proinflammatory cytokines. On the other hand, M1 macrophages will enhance phagocytic activity and improve proinflammatory cytokines generation to accelerate inflammation. On the contrary, M2 macrophages can produce multiple anti-inflammatory cytokines to reduce inflammatory response and promote wound healing (14). It has been proved that wear particles around the prosthesis enhance M1 macrophage expression and augment local inflammation (15). Low expression of M2 phenotype was found in the process. As previously reported M2 macrophages-induced local microenvironment promotes osseointegration and angiogenesis, which is known as osteoimmunology (16–18). Regulation of the macrophage polarization may bring benefits for attenuating wear debris-irritated inflammation (19, 20). As a consequence, it is meaningful to modulate macrophages from M1 phenotypes to M2 phenotypes to reduce debris-irritated osteolysis and strengthen prostheses osseointegration.

Harmine, a β -carboline alkaloid, is primitively extracted from the *Peganum harmala* seeds and then was found in diverse plants, animals and humans (21). It has been reported to have various pharmacological effects on monoamine oxidase action, insulin intake, vasodilatation and cerebral disease (22–25). Harmine has been reported to reduce bone loss of osteoporotic mice and affect bone metabolism. Furthermore, it has been reported that harmine inhibits osteoclast differentiation and bone resorption, promotes osteoblast differentiation through bone morphogenetic protein signaling pathway (26–28). Nevertheless, to this day, the effect of harmine on PPO has not been demonstrated. In addition, the effect of harmine on regulating inflammation and macrophage has not been explored. Besides, whether harmine participates in regulating

macrophage polarization and subsequent osteogenic differentiation in debris-irritated osteolysis remains unknown.

Therefore, the experiment aimed to explore latent immunomodulatory ability of harmine on wear debris-treated macrophages and its succedent effect on osteogenesis. Interestingly, our evidence suggested that harmine administration can alleviate wear-debris-irritated inflammatory response and promote osteogenic differentiation in the conditioned medium. The influence of harmine on macrophage polarization might be the major cause of the immunomodulatory functions. This study suggested that harmine may be a hopeful therapeutic agent to treat PPO.

MATERIALS AND METHODS

Particle Preparation

Ti particles were applied to produce osteolysis and the mean particle size was $1.64 \pm 1.43 \mu\text{m}$ (95% $<4 \mu\text{m}$). For removal of endotoxins, prepared particles were heated at 190°C for 8 h and soaked in 70% ethanol for 2 days. After washing with sterile PBS, the particles were dried for the experiment.

Animals

Experimental procedures stringently followed world admitted principles and gained approval from the ethics committee of our institute. Briefly, forty 7-week-old male C57BL/6 mice were separated at random into four groups (10 per group): the sham operation group (sham), PBS with Ti particles (vehicle), and Ti particles together with low- (5 mg/kg/day) or high- (10 mg/kg/day) concentration of harmine. In this study, PPO model was established by placing Ti particles onto mice calvaria. After anesthetization, a sagittal incision was cut at the medium site of mouse calvaria. The isometric PBS was injected under the periosteum in the sham group and the incision was sutured with no intervention. While in the other groups, 30 mg Ti particles were embedded under the periosteum at middle site of the calvaria. Harmine emulsion was prepared as previously reported (26). On the second day after operation, harmine emulsion at different concentration was intragastrically offered to mice in the low- and high-harmine groups. While in the other groups, mice were treated with isometric volume of emulsion without harmine. After daily administration of harmine for 2 weeks, the calvariae were collected and fixed for subsequent radiological and histological study. Besides, the major organs (liver and kidney) were obtained to evaluate the potential organ damage by harmine. At the same time, the blood samples were collected for biochemical index evaluation.

Microcomputed Tomography (μCT) Analysis

Fixed calvaria were analyzed by μCT (SkyScan, Aartselaar, Belgium). The scanning parameters were set as a resolution of $9 \mu\text{m}$ with X-ray energy of 50 kV and $500 \mu\text{A}$. Three-dimensional (3D) and two-dimensional (2D) images were reconstructed using the manufacturer's software. Then a

columniform region of interest (ROI, $3 \times 3 \times 1$ mm) was drawn at the midline suture center to determine bone mineral density (BMD), number of pores, and bone volume/tissue volume (BV/TV) by analyzer software as described (29).

Histological Analysis, Immunohistochemistry and Immunofluorescence Staining

The fixed calvaria were decalcified and paraffin embedded with the standard procedure. Coronal sections ($5 \mu\text{m}$) were made with a microtome and saved for hematoxylin and eosin (H&E) staining. Section pictures of staining were observed using a high-quality microscope. As previously described, bone thickness was analyzed according to the protocols (30). Masson trichrome (MT) staining kit was used to identify new immature collagen (blue), which indicated new bone and fibrous tissue formation. On the other hand, zones full of mature collagen emerged vivid red. In each section, positive regions were determined microscopically and histomorphometric analysis was performed using a Zeiss microscope by two independent observers.

Immunohistochemistry staining was conducted to identify interleukin (IL)-1 β (1:500), tumor necrosis factor- α (TNF- α , 1:500), IL-6 (1:600), osteocalcin (OCN, 1:100) and Runt-related transcription factor 2 (Runx2, 1:500) (all purchased from Abcam, Cambridge, UK) expression. After antigen retrieval, sections were incubated with respective primary antibodies overnight at 4°C. Then sections were washed followed by 30 min incubation of the secondary antibody at normal temperature. Color was developed using 3, 3'-diaminobenzidine tetrahydrochloride and rinsed sections were counterstained by hematoxylin. The positive cells which appeared brown or yellow in specific regions were counted using a microscope by two independent observers.

Immunofluorescence staining of tissue sections was conducted to evaluate the effect of harmine on macrophage polarization. After antigen retrieval, tissue sections were incubated with antibodies against anti-F4/80 (macrophage, 1:50) and either anti-iNOS (M1 phenotype, 1:100) or anti-Arg-1 (M2 phenotype, 1:1,000) at 4°C overnight. Respective goat anti-rat IgG H&L (Alexa Fluor 488; Abcam) or goat anti-rabbit IgG H&L (Alexa Fluor 647, Abcam) were applied for 30 min incubation at 37°C. DAPI was used to counterstain the nucleus. Finally, confocal microscopic pictures were obtained using a Zeiss laser scanning microscope (LSM 510; Zeiss). Image analysis was performed with the LSM 5 Release 4.2 software.

Cell Culture

Murine macrophage RAW 264.7 cells were cultured in Dulbecco's modified Eagle's medium (DMEM) and pre-osteoblastic MC3T3-E1 cells were cultured in α -modified Eagle's medium (α -MEM), both supplemented with 10% fetal bovine serum (FBS), 1% penicillin and streptomycin in a 90% humidity incubator of 5% CO₂ at 37°C. Cells were added to various plates before treatment without or with Ti particles (0.1 mg/ml) or a mixture of various concentrations of harmine (10 and 50 μM) and Ti particles.

Cell Viability Assay

The proliferation of RAW 264.7 cells was investigated by a cell counting kit-8 (CCK-8) assay. RAW 264.7 cells (1.0×10^4 cells/well) were cultured in triplicate for 48 h. Medium with 10% CCK-8 buffer was applied. The optical density of experimental samples was detected at 450 nm using a microplate-reader (BioTek, Winooski VT, USA) and cell viability was studied. In addition, the cell growth inhibition rate which reflects the extent to which the cell proliferation ability is inhibited compared to the control was converted based on the CCK-8 data (31). In detail, the calculation formula is [growth inhibition rate = $(1 - A_{450 \text{ nm value of the drug group}} / A_{450 \text{ nm value of the control group}}) \times 100\%$].

Immunofluorescence Assay of Macrophage Polarization *In Vitro*

In order to study iNOS and Arg-1 expression by harmine, RAW 264.7 cells were added to 24-well plates (1×10^5 cells/well). Bone marrow derived macrophage cells (BMDM) were also used and isolated from the mice as previously described (32). The cells were both treated with Ti particles with or without various concentrations of harmine (10 and 50 μM) for 24 h. Then cells were fixed by 4% paraformaldehyde at normal temperature. 10% FBS was used to block the nonspecific binding sites. Immunofluorescence assay was then performed according to the identical protocol depicted above.

Nitric Oxide (NO) Production Assay

As described above, Ti particles (0.1 mg/ml) or a mixture of various concentrations of harmine (10 and 50 μM) and Ti particles were added to 24-well plates (1×10^5 cells/well) and cultured for 4 h. NO production in the culture supernatant from each well was measured with a commercial NO assay kit (S0021, Beyotime, Shanghai, China) according to the manufacturer's protocol, which is based on the Griess reaction. In short, 50 μl cell culture medium was mixed with 100 μl Griess reagents I and II at normal temperature in a 96-well plate, and reacted for 10 min. The absorbance was determined by a microplate reader at 540 nm.

Enzyme-Linked Immunosorbent Assay (ELISA)

To better understand the effect of harmine on inflammation, ELISA was conducted to assess the level of inflammatory factors. RAW 264.7 cells were cultured for 96 h and cell medium was centrifuged at 3,000 rpm for 10 min. The supernatants were detected by a standard ELISA kit (R&D systems, Minnesota, USA). The optical densities were determined by a micro ELISA plate reader at 450 nm.

Real-Time Polymerase Chain Reaction (RT-PCR)

Total RNA was collected from cells using the NucleoSpin RNA Kit (MN, Düren, Germany) following the manufacturer's method and reverse-transcribed by the High-Capacity cDNA Reverse Transcription Kit (Applied Biosystems, Foster City, CA, USA). All reactions were run three times independently. In

addition, β -actin was used as the housekeeping gene. The primer sequences in this section were as follows:

CD86 forward 5'-TGGGCGCAGAGAACTTGAT-3' and reverse 5'-AAGCCCGTGTCTTGATCTG-3';
 CD163 forward 5'-GTGGTCAACTCCGCTTGTA-3' and reverse 5'-CTTGGGGCACCATCTGTGAT-3';
 BMP-2 forward 5'-AACGAGAAAAGCGTCAAGCC-3' and reverse 5'-AGGTGCCACGATCCAGTCAT-3';
 VEGF forward 5'-GCAAGAGAAGACACGGTGGT-3' and reverse 5'-CAGGAGGTGGGGTAAGGAG-3';
 OPN forward 5'-CACTCCAATCGTCCCTACAGT-3' and reverse 5'-CTGAAACTCCTAGACTTTGACC-3';
 Runx2 forward 5'-TTGACCTTTGTCCCAATGC-3' and reverse 5'-AGTTGGAGGCACACATAGG-3';
 OCN forward 5'-TTGAAGTGTGTTTTGGACCC-3' and reverse 5'-CCAACAGACACCAGTTGTAAAG-3';
 Osterix forward 5'-TGAGCTGGAACGTCACGTGC-3' and reverse 5'-AAGAGGAGCCAGCCAGACA-3';
 β -actin forward 5'-GTGACGTTGACATCCGTAAAGA-3' and reverse 5'-GTAACAGTCCGCCTAGAAGCAC-3'.

Osteogenic Differentiation Effect of Pre-Osteoblastic MC3T3-E1 Cells in Conditioned Medium (CM)

The conditioned medium was obtained from RAW 264.7 cells in different groups described above. After 4 days of culture in DMEM, the CM from different groups were collected and centrifuged to obtain supernatants. Then the supernatants were mixed with DMEM at a 1:2 ratio. Pre-osteoblastic MC3T3-E1 cells were seeded onto a 24-well plate (5.0×10^4 cells) and cultured in DMEM. And after incubation for 12 h, the medium was replaced by CM for further incubation. Correspondingly, the CM was changed every 48 h.

Alkaline Phosphatase (ALP) Staining

ALP staining of MC3T3-E1 cells in conditioned medium was performed after 7 days of culture. In brief, after 8 min fixation, cells were rinsed and incubated in BCIP/NBT working solution (Beyotime) for 10 min at 37°C. The pictures of staining in culture dishes were obtained.

Alizarin Red S (ARS) Staining

The mineralization of MC3T3-E1 cells was detected by ARS staining. Briefly, MC3T3-E1 cells were cultured in conditioned medium for 21 days and then rinsed with PBS followed by 8 min fixation. Cells were then incubated for 5 min with ARS solution (Cyagen Biosciences). To quantify the mineralization, the stained layers were solubilized with 10% cetylpyridinium chloride (Sigma). Dye absorbance was detected at 490 nm.

Immunofluorescence Staining of Runx2

Pre-osteoblastic MC3T3-E1 cells were cultured in CM and fixed in 4% paraformaldehyde. After 15 min permeabilization by 0.1% Triton-X, cells were blocked by 1% BSA and incubated at 4°C

with Runx2 (1:500, Abcam) antibodies overnight. After washing with PBS, cells were incubated with DY-554 phalloidin. Immunofluorescence assay was then performed according to the identical protocol described above. The confocal microscopic pictures were obtained using a Zeiss laser scanning microscope.

Western Blot Analysis

The RAW264.7 cells (5×10^5 cells/well) were pretreated with 50 μ M harmine for 4 h followed with the addition of Ti particles. Cells were lysed and boiled by sodium dodecyl sulfate (SDS) Lamini buffer. SDS-polyacrylamide gel electrophoresis was performed on 10% polyacrylamide gel and transferred to polyvinylidene fluoride membrane. These antibodies were detected in western blotting: JNK, P-JNK, p65, P-p65, ERK, P-ERK, p38, P-p38, iNOS, CD206 and β -actin (all 1:1,000 dilution, Abcam, UK). The stained protein bands were obtained by an ECL detection kit (Sigma-Aldrich).

Statistical Analysis

SPSS 17.0 software was applied for data analysis. Results were shown as mean \pm SD. The significance of the differences was measured by one-way analysis of variance (ANOVA) with Tukey *post hoc* multiple comparison tests. A *p* value < 0.05 represented statistical significance.

RESULTS

Harmine Alleviated Ti Particle-Induced Osteolysis and Bone Loss *In Vivo*

In order to study the effect of harmine on osteolysis, micro-CT was performed to obtain 3D reconstruction and 2D fault pictures. Micro-CT results showed severe bone resorption distributed mostly at the middle site of calvaria in the Ti group, while there was less in the sham group (**Figure 1A**). In the harmine-treatment groups, debris-irritated osteolysis was alleviated in a dose-dependent manner, whereby less bone resorption was found by treatment of higher concentration of harmine, compared with the low harmine-treatment group. Quantitative analysis showed declines of 60.5% in BMD and 62.5% in BV/TV, and a 3.2-fold increase in the number of pores in the presence of Ti particles compared with the sham group (*p* < 0.01). When harmine was intragastrically administrated at 5 or 10 mg/kg/day, BMD and BV/TV were greatly upregulated compared with the vehicle group (**Figures 1B, C**). Correspondingly, harmine also reduced area of porosity and number of pores (**Figures 1D, E**).

Harmine Reduced the Inflammatory Infiltrate and Cytokines Expression *In Vivo*

To further study the mechanisms underlying the effect of harmine on PPO, wear particle-induced local inflammation and inflammatory cytokines production was measured. Consistent with micro-CT, H&E staining further demonstrated that harmine could inhibit debris-induced bone resorption *in vivo* (**Figure 2A**). Pictures of H&E staining showed few bone pittings in the sham group, whereas clear osteolysis appeared in the vehicle group (**Figure 2A**). In the Ti group, histomorphometric analysis

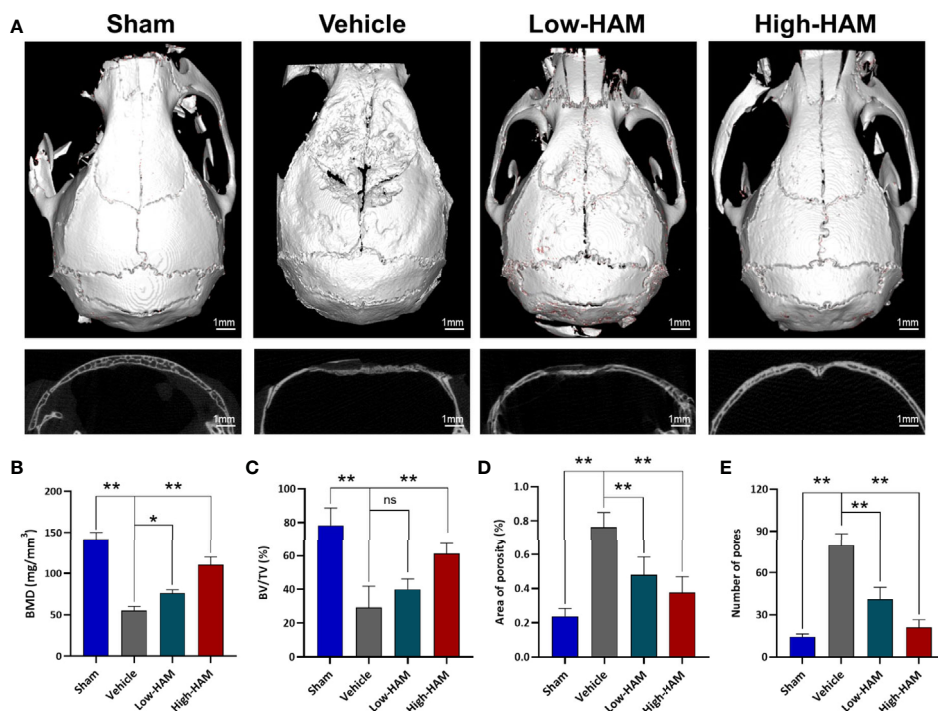


FIGURE 1 | Harmine alleviated Ti debris-stimulated osteolysis and bone loss. **(A)** Representative micro-CT 3D and 2D pictures of murine calvaria. Scale bar indicates 1 mm. Computations for **(B)** BMD, **(C)** BV/TV, **(D)** Area of porosity and **(E)** Number of pores. $n = 3$. All data were expressed as the mean \pm SD, ns, no significance, * $p < 0.05$, ** $p < 0.01$, compared with the vehicle group.

revealed a 62.5% decrease in bone thickness and a 3.9-fold increase in inflammation area, compared with the sham group (Figures 2B, C). Harmine distinctly impacted these Ti-particle-induced effects. In addition, harmine toxicity was not found *in vivo* based on the H&E staining of the major organs and biochemical index evaluation of blood samples (Figure S1). As expected, addition of harmine increased the bone thickness and reduced inflammation area. Immunohistochemical staining of calvarial tissue showed positive stainings for IL-1 β , TNF- α , IL-6 were distributed mainly in the inflammatory cells around the eroded areas (Figures 2D–F). And levels of IL-1 β , TNF- α , and IL-6 were greatly elevated in the presence of Ti particles, compared with the sham group (Figures 2D–I). On the contrary, few positive staining responses for these inflammatory cytokines were observed in the low and high harmine-treatment groups.

Harmino Inhibited Particle-Induced Inflammatory Reactions by Regulating Macrophage Polarization *In Vivo*

Macrophages have the ability to polarize into diverse phenotypes in the multiple microenvironments. Specifically, M1 phenotype is proinflammatory, while M2 phenotype is anti-inflammatory. Considering the vital role of macrophages in the inflammatory response, the relationship between harmine and macrophage polarization was investigated *in vivo*. It turned out that massive M1 phenotype macrophages (F4/80⁺/iNOS⁺, merged as orange)

distributed around the eroded areas in the vehicle group, and just a few expressed the M2 phenotype (F4/80⁺/Arg-1⁺, merged as orange) (Figures 3A, B). Nevertheless, penetration of F4/80⁺/iNOS⁺-positive M1 phenotype macrophages is reversed by harmine and the proportion of anti-inflammatory F4/80⁺/Arg-1⁺-positive M2 phenotype macrophages increases. This indicated harmine treatment shifted the polarization of macrophages from M1 to M2, thereby decreased inflammation in PPO.

Harmino Promotes Osteogenic Formation in the Murine PPO Model

In order to further study whether harmine treatment could enhance osteogenesis ability in Ti-particle-induced osteolysis, masson and immunohistochemical staining was performed to assess osteoblastic bone formation *in vivo*. Ti particles decreased the bone collagen fibers and collagen volume fraction (CVF) (Figures 4A, C). However, treatment of harmine highly improved bone collagen fiber formation and CVF in the presence of Ti particles. Based on the immunohistochemical staining, the level of critical osteogenic differentiation factor of Runx2 was obviously decreased after stimulation of Ti particles compared with the sham group (Figures 4B, D). In detail, 55.4% decline ($p < 0.01$) of Runx2-positive cells number was found by Ti particles (Figure 4D). However, higher expression level of Runx2-positive cells was observed in the harmine-treatment groups, which is consistent with the results of immunohistochemical staining of OCN (Figures 4B, D, E).

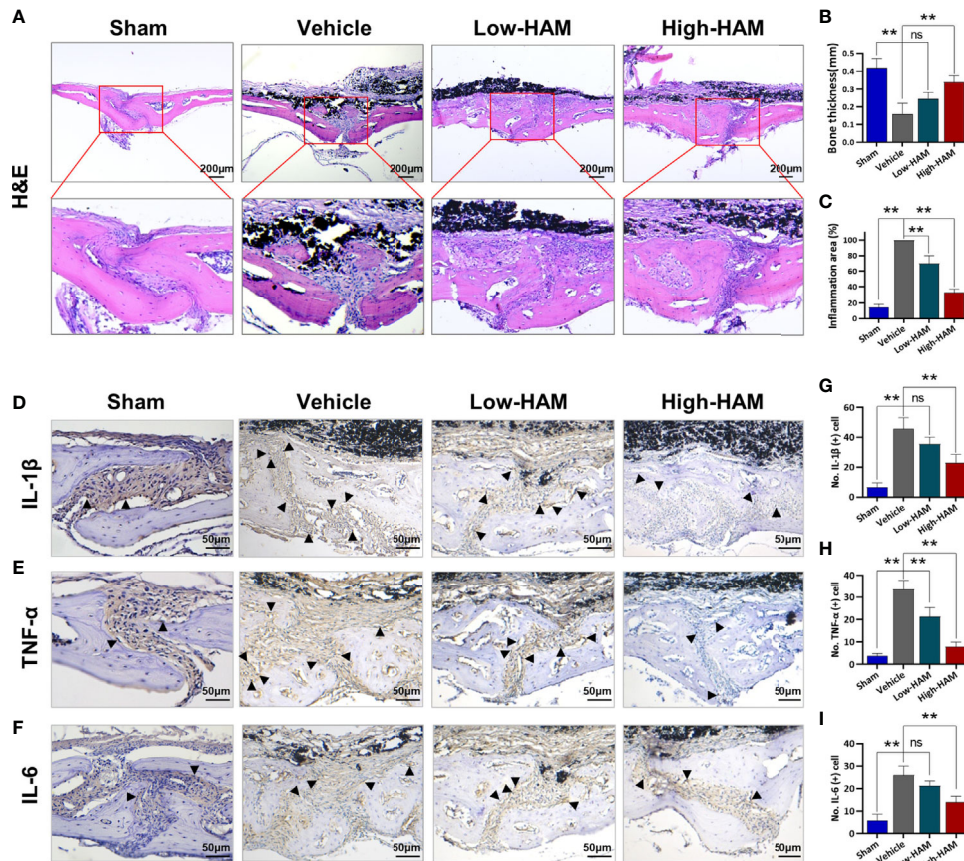


FIGURE 2 | Harmine reduced the inflammatory infiltrate and cytokines expression. **(A)** Histological staining of (H&E). **(B)** Bone thickness. **(C)** Inflammation area. Immunohistochemical staining of inflammatory factors: **(D)** IL-1 β , **(E)** TNF- α , and **(F)** IL-6. Number of positive cells: **(G)** IL-1 β , **(H)** TNF- α , and **(I)** IL-6. Scale bar indicates 200 and 50 μ m. n = 3. All data were expressed as the mean \pm SD, ns, no significance, ***p* < 0.01, compared with the vehicle group.

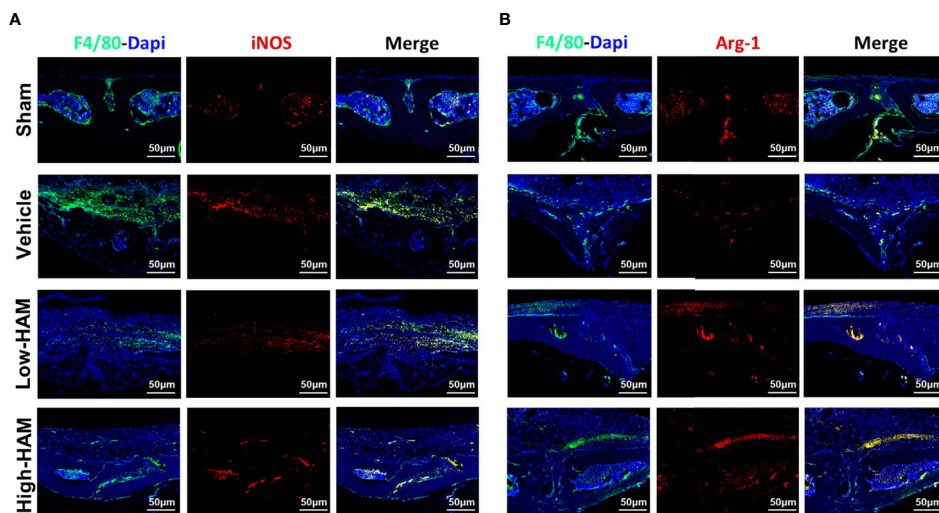


FIGURE 3 | Harmine treatment shifted the polarization of macrophages from M1 to M2 in PPO. Representative immunofluorescent staining images for **(A)** iNOS (M1 marker) and **(B)** Arg-1 (M2 marker). Scale bar indicates 50 μ m. n = 3.

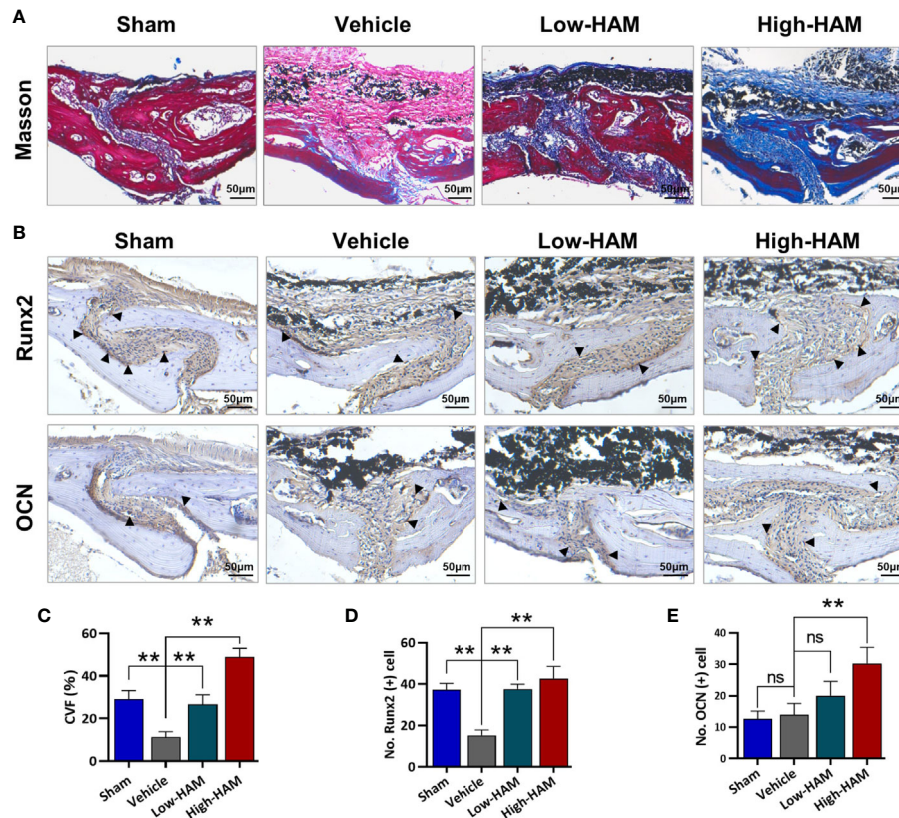


FIGURE 4 | Harmine promoted osteogenic formation in the murine PPO model. **(A)** Histological staining of Masson. **(B)** Immunohistochemical staining of Runx2 and OCN. **(C)** Collagen volume fraction. **(D)** Number of Runx2 positive cells. **(E)** Number of OCN positive cells. Scale bar indicates 50 μ m. $n = 3$. All data were expressed as the mean \pm SD, ns, no significance; ** $p < 0.01$, compared with the vehicle group.

Harmine Promoted the Polarization of Macrophages From M1 to M2 *In Vitro*

CCK-8 assay was conducted and cell growth inhibition rate was obtained to assess toxicity of harmine for RAW264.7 cells. The data showed cell viability was unaffected by treatment with concentrations below 100 μ M of harmine (Figures 5A, B). Cell morphological analysis was performed as shown in Figure 5C. The classical M1 phenotype macrophages are usually flat with multiple synaptic structures, while M2 phenotypes present spindle. In the control group without Ti particles, the majority of RAW264.7 cells appeared small and round. Lipopolysaccharide (LPS) or TNF- α is usually used as an activator of M1 macrophages (32). And the results showed LPS induced multiple M1 phenotype macrophages. And after stimulation of Ti particles, the cells were flat with many synaptic structures, which is like that in LPS group. However, harmine treatment significantly decreased the number of polygonal cells, and cone-shaped cells highly improved by the higher concentration of harmine (Figure 5C).

Immunofluorescence assay was carried out to evaluate the effect of harmine on the activation of macrophages *in vitro*. The results showed Ti particles enhanced the ratio of M1 macrophages (iNOS⁺, red) compared with control group

(RAW in Figure 5D and BMDM in Figure S2). On the contrary, harmine treatment featured a higher expression of the M2 macrophages (Arg-1⁺, red) compared with Ti group (Figure 5D). And the inflammatory NO production in the supernatants was much higher in the Ti group than that in the control group. However, harmine was found to reduce Ti-induced NO production in a dose-dependent manner (Figure 5E). Besides, western blot analysis of RAW264.7 cells revealed that Ti particles stimulation enhanced expression of iNOS (Figure S3). Interestingly, harmine treatment significantly reduced iNOS expression and enhanced CD206 expression compared with that in the Ti group (Figure S3). These data demonstrated that harmine treatment could shift the macrophage from the proinflammatory M1 phenotype to the anti-inflammatory M2 phenotype in line with the histological study as mentioned above.

Cytokine Production and Gene Expression *In Vitro*

As shown in Figures 5F, G, compared with the control group, Ti particle stimulation enhanced the inflammatory cytokine expression of TNF- α and IL-6. However, harmine treatment highly reduced TNF- α and IL-6 expression. On the other

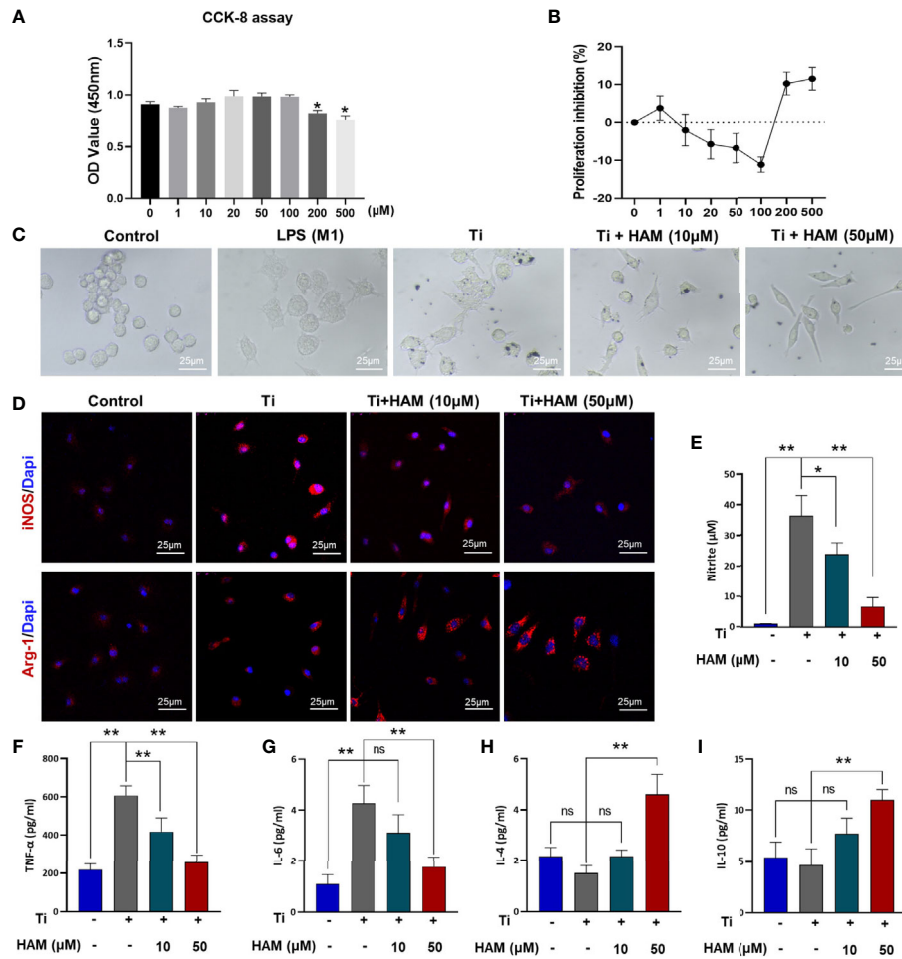


FIGURE 5 | Harmine promoted the polarization of macrophages from M1 to M2 *in vitro*. **(A)** Cell proliferation was evaluated by CCK-8 assay. **(B)** Proliferation inhibition of harmine on RAW macrophages. **(C)** Morphology of RAW macrophages by a light microscope. Scale bar indicates 25 μm. **(D)** Representative immunofluorescent staining images: red (M1 marker: iNOS and M2 marker: Arg-1), and blue (Dapi, directing against nuclei). **(E)** NO content determined by Griess reagent. **(F–I)** Protein level expressions of inflammatory cytokines in Ti particles-treated macrophages (measured by ELISA). Scale bar indicates 25 μm. n = 3. All data were expressed as the mean ± SD, ns, no significance; *p < 0.05, **p < 0.01, compared with the Ti group.

hand, in the high concentration harmine-treatment group, cells expressed the supreme level of IL-4 and IL-10 (Figures 5H, I), which are mostly secreted from M2 macrophages. RT-PCR revealed that after treatment of harmine, CD86 (M1 marker) mRNA level was downregulated compared with the Ti group (Figure 6A). By contrast, CD163 (M2 marker) expression was upregulated in the harmine-treatment groups (Figure 6B). Besides, harmine treatment enhanced BMP-2 and VEGF (bone-related gene) mRNA levels (Figures 6C, D), indicating a potential osteogenic ability with treatment of harmine.

Harmine Suppressed Ti Particle-Induced Activation of JNK *In Vitro*

JNK signaling pathway has been proved to be a critical modulator of macrophage polarization and inflammatory cytokine generation (33). And macrophage polarization is also managed by nuclear factor-κB (NF-κB) (p65, IκBa) (34, 35). In this study,

western blot analysis of RAW264.7 cells revealed that Ti particles stimulation obviously enhanced phosphorylation of JNK and p65 (Figures 6E–G). Interestingly, Ti-particle-induced activation of JNK was suppressed by harmine (Figures 6E, F). However, activation of p65 was unaffected with harmine treatment (Figures 6E, G). To further identify the inhibitory effect of harmine on the JNK signaling pathway, after pre-treatment with harmine for 4 h, cells were stimulated with Ti particles for various times (5, 15, or 30 min). JNK is one of three major mitogen-activated protein kinases (MAPKs) signaling pathways (p38, ERK, and JNK). The data revealed that harmine had no inhibitory effect on p38, ERK and p65 (Figures 6H, J, K and Figure S4). Nevertheless, JNK activation in the presence of Ti particles was significantly inhibited in the harmine treated group (Figures 6H, I). These data indicate that harmine reduced particle-induced inflammation and that JNK might play a central role in this process.

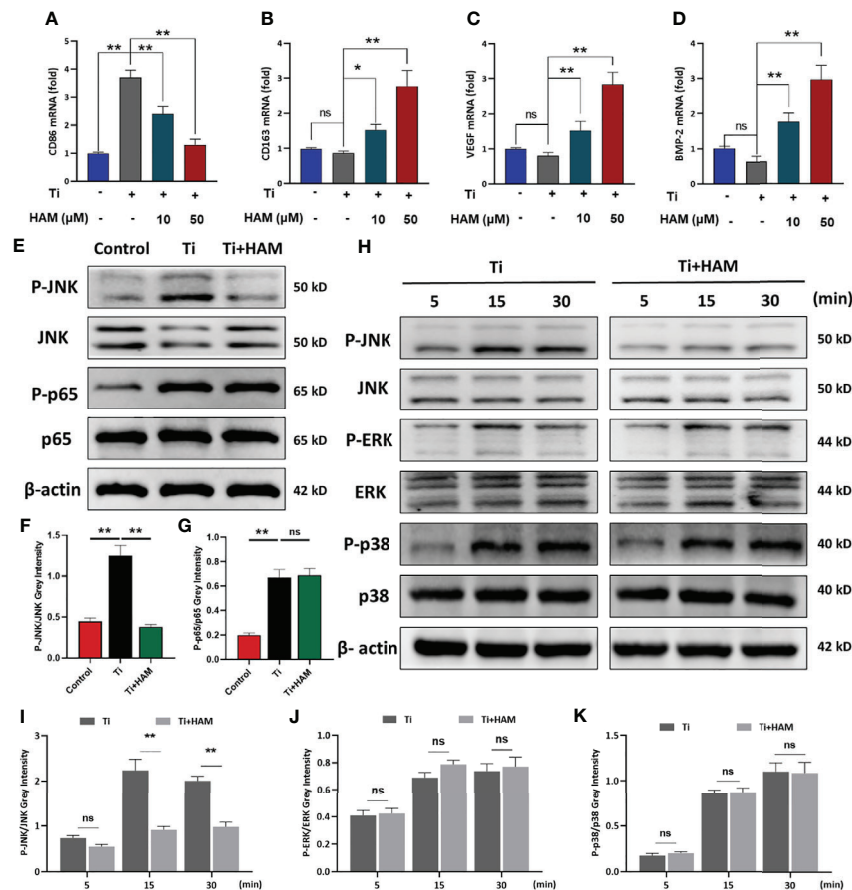


FIGURE 6 | Harmine suppressed Ti particle-induced activation of JNK signaling *in vitro*. RT-PCR results for (A) M1 marker CD86, (B) M2 marker CD163, (C) VEGF and (D) BMP-2. (E) JNK, P-JNK, p65 and P-p65 protein levels, detected by western blot analysis. The relative levels of (F) P-JNK/JNK and (G) P-p65/p65. (H) JNK, P-JNK, ERK, P-ERK, p38 and P-p38 protein levels at various times, detected by western blot analysis. The relative levels of (I) P-JNK/JNK, (J) P-ERK/ERK and (K) P-p38/p38. $n = 3$. All data were expressed as the mean \pm SD, ns, no significance $*p < 0.05$, $**p < 0.01$.

The Assessment of Osteogenic Differentiation Ability in Conditioned Medium

We used the supernatants of RAW264.7 cell culture as conditioned medium to assess immunomodulatory effect of harmine on osteogenic differentiation in MC3T3-E1 cells (Figure 7A). After the cells were cultured in CM, ALP staining and ARS staining were performed as mentioned above. The ALP activity in the CM^{Ti} group was 58.5% ($p < 0.05$) lower than the CM^{Control} group (Figures 7B, C). However, ALP activity was greatly increased in the CM^{Ti + harmine10} and CM^{Ti + harmine50} groups. Meanwhile, ARS staining revealed mineralization was decreased in the CM^{Ti} group (Figures 7D, E). Greater calcium mineralization was observed in the CM^{Ti + harmine50} group, followed by the CM^{Ti + harmine10} group. On the side, immunofluorescence staining was carried out and a similar tendency was found: the CM^{Ti + harmine50} group had the highest expression of Runx2, while the lowest Runx2 expression appeared in the CM^{Ti} group (Figure 7F). Meanwhile, RT-PCR was performed to assess the impact of

CM on osteogenic transcription factors. Similarly, the mRNA levels of OPN, Runx2, OCN and Osterix were decreased in the CM^{Ti} group (Figures 7G–J). However, the CM^{Ti + harmine50} group had a higher mRNA levels of these osteogenic transcription factors.

DISCUSSION

TJA is a well-established effective treatments for terminal joint sickness in past decades. Increasing evidence indicates that wear particles, generated from joint prostheses, can induce a chronic inflammation response by the further recruitment of macrophages, which secrete multiple proinflammatory factors, such as chemokines and cytokines (36, 37). And it has been demonstrated that macrophage polarization exerts great influence in the pathogenesis of inflammatory osteolysis. Therefore, targeted suppression of inflammatory response and macrophage polarization is clearly a potential treatment for alleviating wear-particle-induced bone loss after TJA.

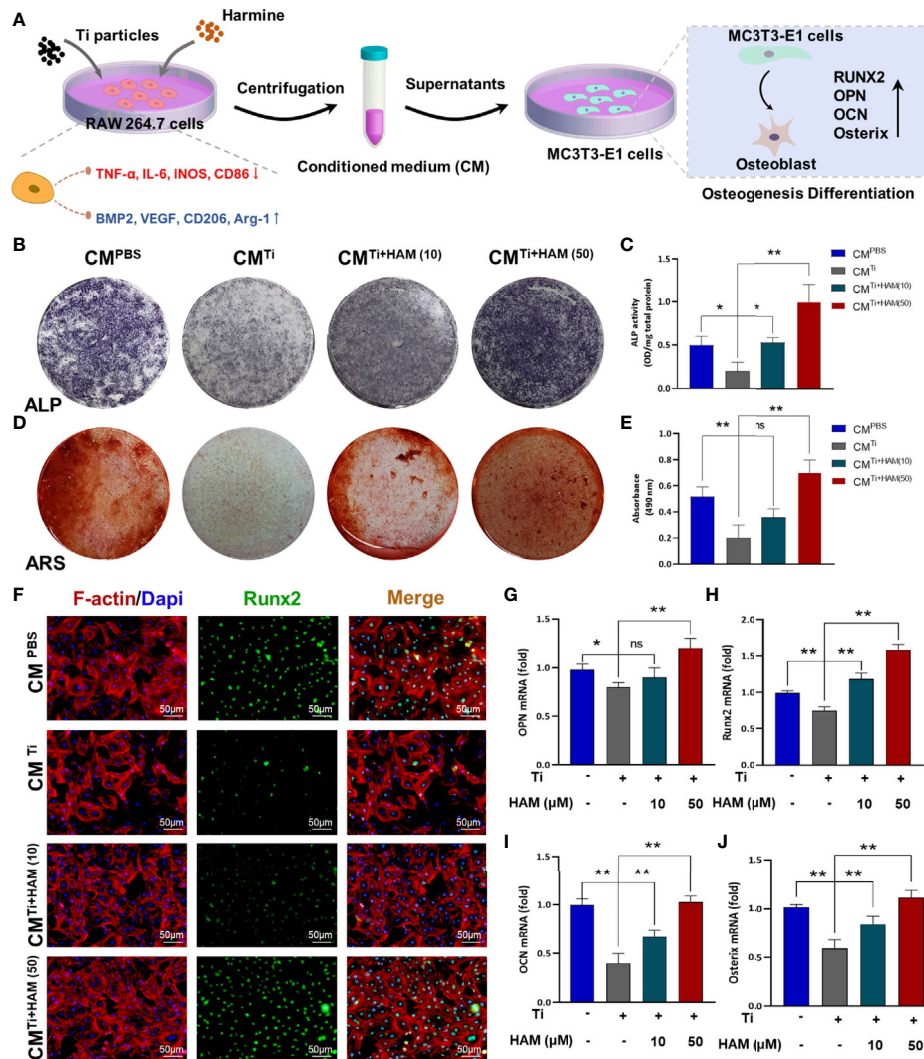


FIGURE 7 | The assessment of osteogenic differentiation ability in conditioned medium. **(A)** Pattern diagram. We used the supernatants of RAW264.7 cell culture as conditioned medium to assess immunomodulatory effect of harmine on osteogenic differentiation in MC3T3-E1 cells. **(B)** ALP staining assessed osteogenic differentiation of MC3T3-E1 cells in different groups. **(C)** ALP activity. **(D)** ARS staining for measuring mineralization of MC3T3-E1 cells from each group. **(E)** Absorbance at 490 nm. **(F)** Images of the MC3T3-E1 cells after coimmunostaining: red (actin rings), green (Runx2) and blue (nuclei). Scale bar indicates 50 μ m. RT-PCR results for **(G)** OPN, **(H)** Runx2, **(I)** OCN and **(J)** Osterix in conditioned medium from different groups. $n = 3$. All data were expressed as the mean \pm SD, ns, no significance; * $p < 0.05$, ** $p < 0.01$, compared with the Ti group.

Recently, harmine, a β -carboline alkaloid, has been reported to reduce bone loss of osteoporotic mice and affect bone metabolism. Furthermore, it has been reported that harmine inhibits osteoclast differentiation and promotes osteoblast differentiation through bone morphogenetic protein signaling pathway (26–28). Moreover, the immunomodulatory effects of harmine have also drawn much attention. Nevertheless, to this day, the effect of harmine on PPO and macrophage polarization has not been demonstrated. So, this experiment was conducted to investigate whether harmine could alleviate debris-irritated bone loss in a murine osteolysis model. As previously reported, Ti particles can induce severe bone destruction in the murine calvaria (38). To our expectation, harmine greatly attenuated the

severity of bone destruction in debris-irritated mice. Micro-CT revealed that BMD and BV/TV were enhanced and porosity was reduced by application of harmine. And histomorphological staining ulteriorly showed that harmine treatment attenuated Ti particle-irritated osteolysis and reduced eroded bone surface. Collectively, these evidences indicated that treatment with harmine might produce an active effect to treat PPO. However, it has been reported that intraperitoneal injection of harmine could bring some side effects (25, 39), which slow the process of harmine toward wider clinical applications. During the experiment, harmine emulsion was used and all the mice oral gavaged with harmine emulsion survived and did not have any side effects. And oral administration is more convenient and

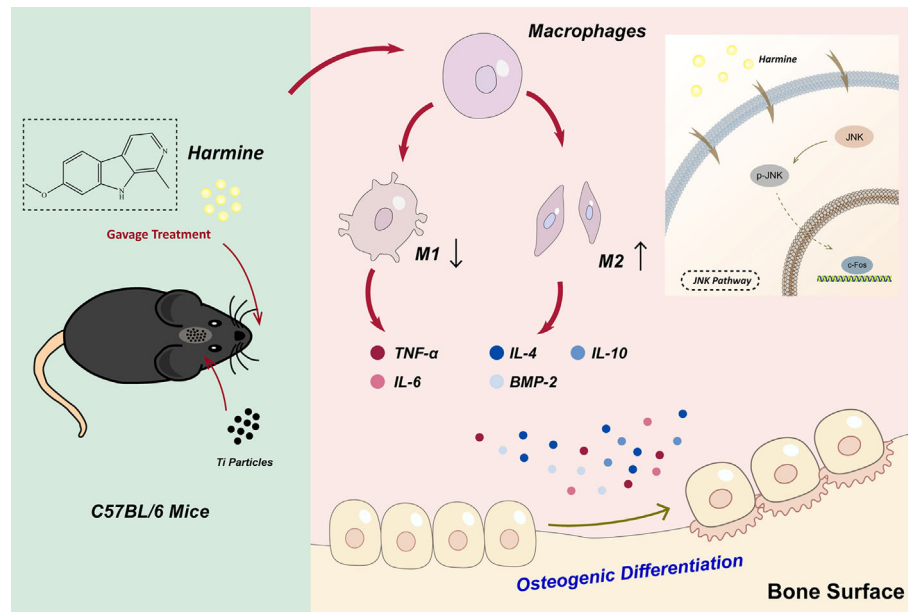


FIGURE 8 | Harmine alleviated the particle-induced inflammation and facilitated the polarization of macrophages from M1 phenotypes to M2 phenotypes by blocking the JNK signaling pathway as well as osteogenic formation *in vitro* and *in vivo*.

acceptable in clinic. Therefore, harmine emulsion may be a hopeful and more secure therapeutic agent for osteolytic disease, which requires verification by future clinical trials.

Macrophages have multiple functions and play an important role in response to microenvironmental signals. For the past few years, the concept of M1 macrophages and M2 macrophages has been built. Specifically, M1 phenotype is proinflammatory, while M2 phenotype is anti-inflammatory (13, 14). Wear particles around the prosthesis have been reported to enhance M1 macrophages expression and lower expression of M2 macrophages. Regulation of the macrophage polarization could bring benefit for attenuating wear debris-irritated inflammation. And whether harmine attenuated Ti particle-irritated osteolysis by regulating macrophage polarization remains unknown. Immunohistochemical staining of calvarial tissue showed the inflammatory cytokines of IL-1 β , TNF- α , and IL-6 were greatly elevated by stimulation of Ti particles. On the contrary, the level of these inflammatory cytokines was lowered with harmine treatment. This indicates that harmine could inhibit particle-induced inflammatory response. As previously described, stimulation of Ti particles enhanced the expression of F4/80⁺/iNOS⁺-positive M1 phenotype and lowered F4/80⁺/Arg-1⁺-positive M2 phenotype expression. Nevertheless, penetration of M1 phenotype macrophages is reversed by harmine and the proportion of anti-inflammatory M2 phenotype macrophages increases. This indicated harmine treatment may shift the polarization of macrophages from M1 to M2, thereby decreased inflammation in PPO. Meanwhile, the effect of harmine on macrophage polarization was investigated *in vitro*. Cell morphological analysis of macrophages revealed that Ti particles induce classical M1 phenotypes with numerous synaptic

structures, while harmine significantly decreased the number of M1 macrophages and increased the number of M2 macrophages, especially in the high-harmine concentration group. In addition, the results of immunofluorescence assay and western blot analysis directly demonstrated that harmine increased Arg-1 level and decreased iNOS level. In addition, variations in proinflammatory and anti-inflammatory cytokines revealed the diversity between M1 and M2 phenotypes. As expected, RT-PCR results were consistent with immunofluorescence results, harmine treatment decreased the mRNA level of CD86 and enhanced CD163 expression. In general, these data demonstrated that harmine could inhibit particle-induced inflammatory response and shift macrophages from proinflammatory M1 phenotypes to anti-inflammatory M2 phenotypes.

As previously reported, unnatural bone remodeling in the inflammatory microenvironment is similarly crucial in particle-irritated bone destruction (40, 41). Increasing evidence have indicated that wear debris can suppress osteogenic differentiation in osteolysis (42, 43). Bone formation plays a critical role in treating osteolytic disease. Low expression of M2 macrophages in the particle-induced inflammatory microenvironment had a negative effect on osseointegration and angiogenesis (16, 17). In this experiment, we proved that harmine could reverse the decline in bone collagen fibers under the particle-stimulated inflammatory condition, and enhance the levels of critical osteogenic differentiation factors of Runx2 and OCN *in vivo*. Besides, BMP-2 and VEGF mRNA levels were also increased in the harmine-treatment groups *in vitro*, indicating a potential osteogenic ability with treatment of harmine. Moreover, ALP staining, ARS staining and immunofluorescence staining of

MC3T3-E1 cells cultured in CM further proved that harmine could promote subsequent osteogenic differentiation capacity in an inflammatory microenvironment. Additionally, the immunomodulatory correlation between macrophage polarization and osteogenesis has been reported to be a critical mechanism involved in bone regeneration (44–46). It has been suggested that harmine could affect bone metabolism as described above. Indeed, the direct relationship between harmine and osteoblastogenesis as well as osteoclastogenesis has not been well understood in PPO, which needs further investigation in future studies.

We subsequently explore the underlying mechanism of harmine-induced suppression on local inflammation as well as regulation of macrophage polarization. It has been proved that M1 phenotype macrophages stimulated by wear particles could produce a continuing inflammatory reaction *via* the JNK signaling pathway (33). The JNK can be phosphorylated and induce downstream gene transcription. As previously described, JNK signaling pathway could be activated in bone marrow-derived macrophages by stimulation of wear debris. JNK is crucial to the activation of the c-jun transcription factor and was reported to accelerate osteoclastogenesis (36, 47). And macrophage polarization is also regulated by NF- κ B signaling pathway (34, 35). Western blotting suggested that JNK might play a central role in regulating macrophage polarization and inflammatory reactions. JNK signaling pathway is usually excited by two upstream mitogen-activated protein kinase kinases (MAP2Ks) (MKK4 and MKK7), which straightly phosphorylate JNK on threonine (Thr183) and tyrosine (Tyr185) residues (48). Besides, MKK4 and MKK7 are activated by upstream pathways *via* multiple mitogen-activated protein kinase kinases (MAP3Ks) (49). Nevertheless, the accurate molecular mechanisms involved in the regulation of inflammation and macrophage polarization by harmine require further investigation in the future.

There were some limitations in our study. First, the murine calvarial model in this experiment produced acute inflammation rather than the chronic inflammation generally existed in aseptic loosening. The osteolysis process was investigated for a short period of 14 days. Then a larger animal model more be more suitable for assessing the long-term efficacy and safety of harmine treatment. Secondly, Ti particles were used in the study rather than ultrahigh molecular weight polyethylene debris, which are the primary materials to induce osteolysis in clinical practice (50). We chose Ti particles here because of their stability and easy adhesion. Ti particles and polyethylene debris have been reported to trigger osteolytic effects comparably (51, 52).

CONCLUSION

In general, this study indicated that in wear debris-irritated inflammatory osteolysis, harmine notably alleviated the particle-induced inflammatory response and shifted macrophage polarization from M1 phenotype to M2 phenotype as well

as osteogenic formation *in vitro* and *in vivo*. And the immunomodulatory ability of harmine might be attributed to the suppression of JNK signaling pathway (**Figure 8**). In addition, the findings demonstrated for the first time that harmine exerts a protective influence on a murine PPO model. All the results strongly show that harmine can be a promising therapeutic agent to treat PPO.

DATA AVAILABILITY STATEMENT

The original contributions presented in the study are included in the article/**Supplementary Material**. Further inquiries can be directed to the corresponding authors.

ETHICS STATEMENT

The animal study was reviewed and approved by Ethics committee of Changzhou No. 2 Hospital.

AUTHOR CONTRIBUTIONS

LW conducted all the experiments with assistance from the other authors. GG, WW and QW assisted in the surgical procedure of establishing murine calvarial osteolysis model and biochemical analysis. NX and GG performed the histological staining and analysis. DZ and SJ performed the cell culturing, differentiation, qRT-PCR and western blot assay *in vitro*. GZ conducted the Micro-CT scanning and reconstruction analysis. YX oversaw the experiments. YW and RZ provided academic guidance suggestions. DG wrote the manuscript with contributions from LW and QW. All authors contributed to the article and approved the submitted version.

FUNDING

This research was supported by the National Natural Science Foundation of China (82002321, 82072425, 81873991), the Social Development Project of Jiangsu Province (BE2015632), the Jiangsu Provincial Medical Youth Talent (QNRC2016751), the Natural Science Foundation of Jiangsu province (BK20180001), and Special Project of Diagnosis and Treatment for Clinical Diseases of Suzhou (LCZX202003).

SUPPLEMENTARY MATERIAL

The Supplementary Material for this article can be found online at: <https://www.frontiersin.org/articles/10.3389/fimmu.2021.657687/full#supplementary-material>

REFERENCES

- Kurtz SM, Ong KL, Schmier J, Zhao K, Mowat F, Lau E. Primary and Revision Arthroplasty Surgery Caseloads in the United States From 1990 to 2004. *J Arthroplasty* (2009) 24(2):195–203. doi: 10.1016/j.arth.2007.11.015
- Price AJ, Alvand A, Troelsen A, Katz JN, Hooper G, Gray A, et al. Knee Replacement. *Lancet (London England)* (2018) 392(10158):1672–82. doi: 10.1016/S0140-6736(18)32344-4
- Gallo J, Goodman SB, Konttinen YT, Wimmer MA, Holinka M. Osteolysis Around Total Knee Arthroplasty: A Review of Pathogenetic Mechanisms. *Acta Biomater* (2013) 9(9):8046–58. doi: 10.1016/j.actbio.2013.05.005
- Kurtz SM, Ong KL, Lau E, Bozic KJ. Impact of the Economic Downturn on Total Joint Replacement Demand in the United States: Updated Projections to 2021. *J Bone Joint Surg* (2014) 96(8):624–30. doi: 10.2106/JBJS.M.00285
- Meffah M, Klingenstein GG, Yun RJ, Ranawat AS, Ranawat CS. Long-Term Performance of Ceramic and Metal Femoral Heads on Conventional Polyethylene in Young and Active Patients: A Matched-Pair Analysis. *J Bone Joint Surg* (2013) 95(13):1193–7. doi: 10.2106/JBJS.L.00432
- Zawawi MS, Perilli E, Stansborough RL, Marino V, Cantley MD, Xu J, et al. Caffeic Acid Phenethyl Ester Abrogates Bone Resorption in a Murine Calvarial Model of Polyethylene Particle-Induced Osteolysis. *Calcif Tissue Int* (2015) 96(6):565–74. doi: 10.1007/s00223-015-9982-8
- Nich C, Rao AJ, Valladares RD, Li C, Christman JE, Antonios JK, et al. Role of Direct Estrogen Receptor Signaling in Wear Particle-Induced Osteolysis. *Biomaterials* (2013) 34(3):641–50. doi: 10.1016/j.biomaterials.2012.10.030
- Nich C, Takakubo Y, Pajarinen J, Ainola M, Salem A, Sillat T, et al. Macrophages-Key Cells in the Response to Wear Debris From Joint Replacements, Journal of Biomedical Materials Research. *Part A* (2013) 101(10):3033–45. doi: 10.1002/jbm.a.34599
- Ingham E, Fisher J. The Role of Macrophages in Osteolysis of Total Joint Replacement. *Biomaterials* (2005) 26(11):1271–86. doi: 10.1016/j.biomaterials.2004.04.035
- Pajarinen J, Kouri VP, Jämsen E, Li TF, Mandelin J, Konttinen YT. The Response of Macrophages to Titanium Particles is Determined by Macrophage Polarization. *Acta Biomater* (2013) 9(11):9229–40. doi: 10.1016/j.actbio.2013.06.027
- Li B, Hu Y, Zhao Y, Cheng M, Qin H, Cheng T, et al. Curcumin Attenuates Titanium Particle-Induced Inflammation by Regulating Macrophage Polarization in Vitro and In Vivo. *Front Immunol* (2017) 8:55. doi: 10.3389/fimmu.2017.00055
- Bai J, Wang H, Chen H, Ge G, Wang M, Gao A, et al. Biomimetic Osteogenic Peptide With Mussel Adhesion and Osteoimmunomodulatory Functions to Ameliorate Interfacial Osseointegration Under Chronic Inflammation. *Biomaterials* (2020) 255:120197. doi: 10.1016/j.biomaterials.2020.120197
- Mills CD, Kincaid K, Alt JM, Heilman MJ, Hill AM. M-1/M-2 Macrophages and the Th1/Th2 Paradigm. *J Immunol (Baltimore Md: 1950)* (2000) 164(12):6166–73. doi: 10.4049/jimmunol.164.12.6166
- Martinez FO, Helming L, Gordon S. Alternative Activation of Macrophages: An Immunologic Functional Perspective. *Annu Rev Immunol* (2009) 27:451–83. doi: 10.1146/annurev.immunol.021908.132532
- Rao AJ, Gibon E, Ma T, Yao Z, Smith RL, Goodman SB. Revision Joint Replacement, Wear Particles, and Macrophage Polarization. *Acta Biomater* (2012) 8(7):2815–23. doi: 10.1016/j.actbio.2012.03.042
- Ono T, Takayanagi H. Osteoimmunology in Bone Fracture Healing. *Curr Osteoporos Rep* (2017) 15(4):367–75. doi: 10.1007/s11914-017-0381-0
- Takayanagi H. Osteoimmunology: Shared Mechanisms and Crosstalk Between the Immune and Bone Systems, Nature Reviews. *Immunology* (2007) 7(4):292–304. doi: 10.1038/nri2062
- Takayanagi H. Osteoimmunology in 2014: Two-faced Immunology-From Osteogenesis to Bone Resorption, Nature Reviews. *Rheumatology* (2015) 11(2):74–6. doi: 10.1038/nrrheum.2014.219
- Antonios JK, Yao Z, Li C, Rao AJ, Goodman SB. Macrophage Polarization in Response to Wear Particles In Vitro. *Cell Mol Immunol* (2013) 10(6):471–82. doi: 10.1038/cmi.2013.39
- Wang Y, Wu NN, Mou YQ, Chen L, Deng ZL. Inhibitory Effects of Recombinant IL-4 and Recombinant IL-13 on UHMWPE-induced Bone Destruction in the Murine Air Pouch Model. *J Surg Res* (2013) 180(2):e73–81. doi: 10.1016/j.jss.2012.04.016
- Patel K, Gadewar M, Tripathi R, Prasad SK, Patel DK. A Review on Medicinal Importance, Pharmacological Activity and Bioanalytical Aspects of Beta-Carboline Alkaloid “Harmine”. *Asian Pac J Trop Biomed* (2012) 2(8):660–4. doi: 10.1016/S2221-1691(12)60116-6
- Cao R, Peng W, Wang Z, Xu A. beta-Carboline Alkaloids: Biochemical and Pharmacological Functions. *Curr Med Chem* (2007) 14(4):479–500. doi: 10.2174/092986707779940998
- Waki H, Park KW, Mitro N, Pei L, Damoiseaux R, Wilpitz DC, et al. The Small Molecule Harmine is an Antidiabetic Cell-Type-Specific Regulator of PPARgamma Expression. *Cell Metab* (2007) 5(5):357–70. doi: 10.1016/j.cmet.2007.03.010
- Berrougui H, Martín-Cordero C, Khalil A, Hmamouchi M, Ettaib A, Marhuenda E, et al. Vasorelaxant Effects of Harmine and Harmaline Extracted From Peganum Harmala L. Seeds in Isolated Rat Aorta. *Pharmacol Res* (2006) 54(2):150–7. doi: 10.1016/j.phrs.2006.04.001
- Aricioglu F, Yillar O, Korcegez E, Berkman K. Effect of Harmine on the Convulsive Threshold in Epilepsy Models in Mice. *Ann New York Acad Sci* (2003) 1009:190–5. doi: 10.1196/annals.1304.023
- Huang J, Yin H, Rao SS, Xie PL, Cao X, Rao T, et al. Harmine Enhances Type H Vessel Formation and Prevents Bone Loss in Ovariectomized Mice. *Theranostics* (2018) 8(9):2435–46. doi: 10.7150/thno.22144
- Yonezawa T, Lee JW, Hibino A, Asai M, Hojo H, Cha BY, et al. Harmine Promotes Osteoblast Differentiation Through Bone Morphogenetic Protein Signaling. *Biochem Biophys Res Commun* (2011) 409(2):260–5. doi: 10.1016/j.bbrc.2011.05.001
- Yonezawa T, Hasegawa S, Asai M, Ninomiya T, Sasaki T, Cha BY, et al. Harmine, a β -Carboline Alkaloid, Inhibits Osteoclast Differentiation and Bone Resorption In Vitro and In Vivo. *Eur J Pharmacol* (2011) 650(2-3):511–8. doi: 10.1016/j.ejphar.2010.10.048
- Yang H, Xu Y, Zhu M, Gu Y, Zhang W, Shao H, et al. Inhibition of Titanium-Particle-Induced Inflammatory Osteolysis After Local Administration of Dopamine and Suppression of Osteoclastogenesis Via D2-like Receptor Signaling Pathway. *Biomaterials* (2016) 80:1–10. doi: 10.1016/j.biomaterials.2015.11.046
- Parfitt AM, Drezner MK, Glorieux FH, Kanis JA, Malluche H, Meunier PJ, et al. Bone Histomorphometry: Standardization of Nomenclature, Symbols, and Units. Report of the ASBMR Histomorphometry Nomenclature Committee. *J Bone Miner Res* (1987) 2(6):595–610. doi: 10.1002/jbmr.5650020617
- Xiong L, Liu Y, Zhu F, Lin J, Wen D, Wang Z, et al. Acetyl-11-Keto- β -Boswellic Acid Attenuates Titanium Particle-Induced Osteogenic Inhibition Via Activation of the GSK-3 β /Catenin Signaling Pathway. *Theranostics* (2019) 9(24):7140–55. doi: 10.7150/thno.35988
- Zhu M, Yu B, Bai J, Wang X, Guo X, Liu Y, et al. Cannabinoid Receptor 2 Agonist Prevents Local and Systemic Inflammatory Bone Destruction in Rheumatoid Arthritis. *J Bone Miner Res* (2019) 34(4):739–51. doi: 10.1002/jbmr.3637
- Weavers H, Evans IR, Martin P, Wood W. Corpse Engulfment Generates a Molecular Memory That Primes the Macrophage Inflammatory Response. *Cell* (2016) 165(7):1658–71. doi: 10.1016/j.cell.2016.04.049
- Zhong Z, Umemura A, Sanchez-Lopez E, Liang S, Shalpour S, Wong J, et al. NF-kB Restricts Inflammation Activation Via Elimination of Damaged Mitochondria. *Cell* (2016) 164(5):896–910. doi: 10.1016/j.cell.2015.12.057
- Yu B, Bai J, Shi J, Shen J, Guo X, Liu Y, et al. MiR-106b Inhibition Suppresses Inflammatory Bone Destruction of Wear Debris-Induced Periprosthetic Osteolysis in Rats. *J Cell Mol Med* (2020) 24(13):7490–503. doi: 10.1111/jcmm.15376
- Wang L, Guo X, Zhou W, Ding Y, Shi J, Wu X, et al. Protein Phosphatase 2A as a New Target for Downregulating Osteoclastogenesis and Alleviating Titanium Particle-Induced Bone Resorption. *Acta Biomater* (2018) 73:488–99. doi: 10.1016/j.actbio.2018.04.013
- Catelas I, Jacobs JJ. Biologic Activity of Wear Particles. *Instr Course Lect* (2010) 59:3–16.
- Wang L, Bai J, Wang Q, Ge G, Lin J, Xu N, et al. Inhibition of Protein Phosphatase 2A Attenuates Titanium-Particle Induced Suppression of Bone Formation. *Int J Biol Macromol* (2020) 142:142–51. doi: 10.1016/j.ijbiomac.2019.09.084
- Guan Y, Louis ED, Zheng W. Toxicokinetics of Tremorogenic Natural Products, Harmine and Harmine, in Male Sprague-Dawley Rats, Journal of

- Toxicology and Environmental Health. *Part A* (2001) 64(8):645–60. doi: 10.1080/152873901753246241
40. Bartell SM, Kim HN, Ambrogini E, Han L, Iyer S, Serra Ucer S, et al. Foxo Proteins Restrain Osteoclastogenesis and Bone Resorption by Attenuating H₂O₂ Accumulation. *Nat Commun* (2014) 5:3773. doi: 10.1038/ncomms4773
 41. Park-Min KH, Lim E, Lee MJ, Park SH, Giannopoulou E, Yarilina A, et al. Inhibition of Osteoclastogenesis and Inflammatory Bone Resorption by Targeting BET Proteins and Epigenetic Regulation. *Nat Commun* (2014) 5:5418. doi: 10.1038/ncomms6418
 42. Harris WH. Wear and Periprosthetic Osteolysis: The Problem. *Clin Orthop Relat Res* (2001) 393:66–70. doi: 10.1097/00003086-200112000-00007
 43. Lohmann CH, Dean DD, Köster G, Casasola D, Buchhorn GH, Fink U, et al. Ceramic and PMMA Particles Differentially Affect Osteoblast Phenotype. *Biomaterials* (2002) 23(8):1855–63. doi: 10.1016/S0142-9612(01)00312-X
 44. Saldaña L, Vallés G, Bensiamar F, Mancebo FJ, García-Rey E, Vilaboa N. Paracrine Interactions Between Mesenchymal Stem Cells and Macrophages are Regulated by 1,25-Dihydroxyvitamin D₃. *Sci Rep* (2017) 7(1):14618. doi: 10.1038/s41598-017-15217-8
 45. Pan H, Xie Y, Zhang Z, Li K, Hu D, Zheng X, et al. Immunomodulation Effect of a Hierarchical Macropore/Nanosurface on Osteogenesis and Angiogenesis. *Biomed Mater (Bristol England)* (2017) 12(4):045006. doi: 10.1088/1748-605X/aa6b7c
 46. Li H, Lu Y, Qian J, Zheng Y, Zhang M, Bi E, et al. Human Osteoclasts are Inducible Immunosuppressive Cells in Response to T Cell-Derived IFN- γ and CD40 Ligand In Vitro. *J Bone Miner Res* (2014) 29(12):2666–75. doi: 10.1002/jbmr.2294
 47. Rakshit DS, Ly K, Sengupta TK, Nestor BJ, Sculco TP, Ivashkiv LB, et al. Wear Debris Inhibition of Anti-Osteoclastogenic Signaling by Interleukin-6 and Interferon-Gamma. Mechanistic Insights and Implications for Periprosthetic Osteolysis. *J Bone Joint Surg* (2006) 88(4):788–99. doi: 10.2106/JBJS.E.00711
 48. Bubici C, Papa S. JNK Signalling in Cancer: in Need of New, Smarter Therapeutic Targets. *Br J Pharmacol* (2014) 171(1):24–37. doi: 10.1111/bph.12432
 49. Kyriakis JM, Avruch J. Mammalian Mitogen-Activated Protein Kinase Signal Transduction Pathways Activated by Stress and Inflammation. *Physiol Rev* (2001) 81(2):807–69. doi: 10.1152/physrev.2001.81.2.807
 50. Qu S, Bai Y, Liu X, Fu R, Duan K, Weng J. Study on In Vitro Release and Cell Response to Alendronate Sodium-Loaded Ultrahigh Molecular Weight Polyethylene Loaded With Alendronate Sodium Wear Particles to Treat the Particles-Induced Osteolysis. *J Biomed Mater Res Part A* (2013) 101(2):394–403. doi: 10.1002/jbm.a.34327
 51. von Knoch M, Jewison DE, Sibonga JD, Sprecher C, Morrey BF, Loer F, et al. The Effectiveness of Polyethylene Versus Titanium Particles in Inducing Osteolysis In Vivo. *J Orthop Res* (2004) 22(2):237–43. doi: 10.1016/j.orthres.2003.08.013
 52. Wooley PH, Morren R, Andary J, Sud S, Yang SY, Mayton L, et al. Inflammatory Responses to Orthopaedic Biomaterials in the Murine Air Pouch. *Biomaterials* (2002) 23(2):517–26. doi: 10.1016/S0142-9612(01)00134-X

Conflict of Interest: The authors declare that the research was conducted in the absence of any commercial or financial relationships that could be construed as a potential conflict of interest.

Copyright © 2021 Wang, Wang, Wang, Ge, Xu, Zheng, Jiang, Zhao, Xu, Wang, Zhu and Geng. This is an open-access article distributed under the terms of the Creative Commons Attribution License (CC BY). The use, distribution or reproduction in other forums is permitted, provided the original author(s) and the copyright owner(s) are credited and that the original publication in this journal is cited, in accordance with accepted academic practice. No use, distribution or reproduction is permitted which does not comply with these terms.